Journal of Applied Physics

RESEARCH ARTICLE | MAY 10 2022

Compensation of *p*-type doping in Al-doped 4H-SiC

Special Collection: Defects in Semiconductors 2022

Yuanchao Huang ; Rong Wang ; Yiqiang Zhang; Deren Yang ; Xiaodong Pi

J. Appl. Phys. 131, 185703 (2022)
https://doi.org/10.1063/5.0085510

11 April 2024 12:47:02

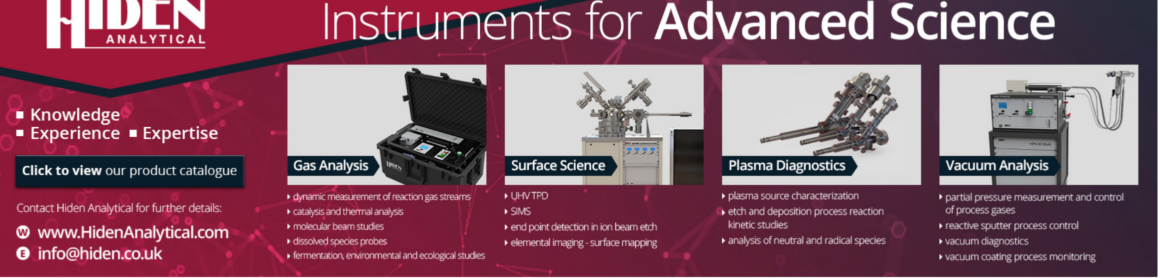

AIP Publishing

Journal of Applied Physics

ARTICLE

scitation.org/journal/jap

Compensation of *p*-type doping in Al-doped 4H-SiC

Cite as: J. Appl. Phys. **131**, 185703 (2022); doi: 10.1063/5.0085510
Submitted: 17 January 2022 · Accepted: 21 April 2022 ·
Published Online: 10 May 2022

View Online

Export Citation

CrossMark

Yuanchao Huang,[1,2] Rong Wang,[2,a)] Yiqiang Zhang,[3] Deren Yang,[1,2] and Xiaodong Pi[1,2,a)]

AFFILIATIONS

[1]State Key Laboratory of Silicon Materials and School of Materials Science and Engineering, Zhejiang University, Hangzhou 310027, China
[2]Institute of Advanced Semiconductors and Zhejiang Provincial Key Laboratory of Power Semiconductor Materials and Devices, Hangzhou Innovation Center, Zhejiang University, Hangzhou 310027, China
[3]School of Materials Science and Engineering and College of Chemistry, Zhengzhou University, Zhengzhou, Henan 450001, China

Note: This paper is part of the Special Topic on Defects in Semiconductors.
[a)]**Authors to whom correspondence should be addressed:** rong_wang@zju.edu.cn and xdpi@zju.edu.cn

ABSTRACT

One of the major challenges of 4H-silicon carbide (4H-SiC) is that the preparation of low resistivity *p*-type 4H-SiC single crystals lags seriously behind that of low resistivity *n*-type 4H-SiC single crystals, hindering the development of important 4H-SiC power devices such as n-channel insulated gate bipolar transistors. In particular, the resistivity of *p*-type 4H-SiC single crystals prepared through the physical vapor transport technique can only be lowered to around 100 mΩ cm. One of the key causes is the incomplete ionization of the *p*-type dopant Al with an ionization energy ∼0.23 eV. Another factor is the compensating effect. It cannot simply assume nitrogen (N) is the sole compensatory center, since the number of the compensating center is larger than the concentration of N doping. In this work, we systematically investigate the compensation of native defects and self-compensation in Al-doped 4H-SiC. It is found that the positively charged carbon vacancies (V_C^{2+}) are also the dominant compensating centers in Al-doped 4H-SiC. When the Al concentration is in the range of 10^{16}–10^{19} cm^{-3}, the concentration of holes is lower by one order of magnitude than the Al concentration because of the compensation of V_C^{2+}. As the Al concentration exceeds 10^{20} cm^{-3}, the concentration of holes is only in the order of magnitude of 10^{19} cm^{-3} owing to the dominant compensation of V_C^{2+} and supplementary self-compensation of interstitial Al (Al_i^{3+}). We propose that the passivation of V_C^{2+} as well as quenching is effective to enhance the hole concentration of Al-doped 4H-SiC.

Published under an exclusive license by AIP Publishing. https://doi.org/10.1063/5.0085510

11 April 2024 12:47:02

I. INTRODUCTION

With the rapid development of power electronics, 4H-silicon carbide (4H-SiC) has been attracting great attention owning to its unique physical properties such as wide bandgap, high breakdown electric field strength, and high thermal conductivity.[1–3] Compared with traditional Si power devices, 4H-SiC power devices such as Schottky barrier diodes (SBDs) and metal–oxide–semiconductor field effect transistors (MOSFETs) possess advantages of higher frequency, higher power-conversion efficiency, lower power loss, and smaller size.[4–10] More significantly, 4H-SiC-based bipolar devices such as gate turn-off thyristors (GTOs) and insulated gate bipolar transistors (IGBTs) hold great promise for ultrahigh voltage (>10 KV) applications, which exceed the working scope of Si-based power devices.[10–15] Current GTOs and IGBTs are fabricated on *n*-type 4H-SiC substrates with very low resistivity, which lead to *p*-channel devices. Since the mobility of electrons is much higher than that of holes in 4H-SiC, *n*-channel power devices may have better performance than *p*-channel power devices.[14,15] However, the development of *n*-channel IGBT has significantly lagged behind that of *p*-channel power devices because it is rather difficult to obtain *p*-type 4H-SiC substrates with very low resistivity. At present, researchers have developed an inverted-growth process that, in principle, could allow all critical epilayers (*p*-type 4H-SiC) to be grown in a continuous sequence on an original *n*-type substrate (∼400 μm), which is subsequently removed by polishing.[15] A *p*-type 4H-SiC

Published under an exclusive license by AIP Publishing

substrates with very low resistivity will be helpful for researchers to fabricate *n*-channel power devices in a direct-growth process.

Until now, the resistivity of *p*-type 4H-SiC single crystals with low resistivity that are still in the research stage has not been reduced below 30 mΩ cm.[16–22] In particular, the resistivity of *p*-type 4H-SiC single crystals prepared via the (physical vapor transport) PVT method can only be reduced to about 100 mΩ cm.[19–22] One of the major reasons is the incomplete ionization of the *p*-type dopant Al. Among all group-III elements, Al has been found to be the best *p*-type dopant in 4H-SiC, but the ionization energy of Al in 4H-SiC is still high, ∼0.23 eV, which leads to the acceptor's ionization rate only about 5%–30% at room temperature.[23,24] Another reason is the compensation effect.[25–30] Presently, it is commonly assumed that nitrogen (N) is the principal compensating center.[25,26] Several experiments, however, indicate there is an additional compensating center in *p*-type SiC because the number of the compensating center is more than the concentration of N doping. Krieger *et al.* grew a bulk crystal of 6H-SiC using PVT with an Al doping concentration of $\sim 1.6 \times 10^{19}$ cm^{-3}. The concentration of the compensating center is 4.0×10^{18} cm^{-3} identified by the Hall effect measurements, which is higher than the N doping concentration (3.0×10^{18} cm^{-3}) measured by secondary ion mass spectroscopy (SIMS).[25] A similar phenomenon is seen in Al-doped *p*-type 4H-SiC epilayers synthesized through chemical vapor deposition (CVD). Asada *et al.* grew Al-doped *p*-type 4H-SiC epilayers with a density of acceptors of about 7.1×10^{18} cm^{-3} and a compensating center density of approximately 1.2×10^{16} cm^{-3}. SIMS measurements indicate that the N doping concentration is less than 5.0×10^{15} cm^{-3}, which is an order of magnitude less than the compensating center.[27] All of these experiments suggest the existence of an additional compensating center, but the mechanism by which this compensation occurs remains unclear. Carbon vacancies (V_C) and V_C-related defects are widely considered to be the principal compensating center in Al implanted *p*-type SiC.[28–30] This is because co-implanting Al and C may enhance the concentration of free holes by a factor of 1.5–2.5.[28] At the moment, it is unknown if V_C serves as a compensating center for the as-grown Al-doped *p*-type SiC.

In this work, we systemically investigate the compensation mechanisms of *p*-type doping in as-grown Al-doped 4H-SiC. The compensation of native defects and the self-compensation of interstitial Al (Al_i) are revealed in the framework of first-principles calculations. It is found that the positively charged carbon vacancies (V_C^{2+}) are the dominant compensating centers in Al-doped 4H-SiC. When the Al concentration is in the range of 10^{16}–10^{19} cm^{-3}, the concentration of holes is lower by one order of magnitude than the Al concentration because of the compensation of V_C^{2+}. As the Al concentration exceeds 10^{20} cm^{-3}, the concentration of holes is only in the order of magnitude of 10^{19} cm^{-3} owing to the dominant compensation of V_C^{2+} and supplementary self-compensation of interstitial Al_i^{3+}. The hole concentration of Al in 4H-SiC substrate and epilayer can be significantly improved with the passivation of V_C^{2+} and quenching.

II. COMPUTATIONAL METHODS

A. First-principles calculations

First-principles calculations are performed using the projector-augmented wave (PAW) method implanted in the Vienna *ab initio* Simulation Package (VASP). The wave functions are expanded by using the plane wave energy cutoff of 500 eV. The Perdew–Burke–Ernzerhof (PBE) functional with the generalized gradient approximation (GGA) exchange correlation is employed to describe the exchange–correlation interactions.[31] Brillouin-zone integrations are approximated by using special *k*-point sampling of the Monkhorst–Pack scheme with a *k*-point mesh of $2 \times 2 \times 2$. The supercell lattice and atomic coordinates are fully relaxed until the total energy per cell and the force on each atom are less than 1.0×10^{-6} eV and 0.01 eV/Å, respectively. The screened hybrid density functional of Heyd, Scuseria, and Ernzerhof (HSE06) is adopted to calculate the electronic properties of 4H-SiC. Defects are modeled in a $6 \times 6 \times 2$ supercell of 4H-SiC with 576 atoms. The calculated lattice parameters of 4H-SiC are $a = 3.07$ Å and $c = 10.05$ Å. The calculated bandgap energy of 4H-SiC is 3.18 eV, which agrees well with experimental results.[1]

B. Defect formation calculations

The formation energy of a defect α at the charge state q in 4H-SiC is calculated by using[32,33]

$$\Delta H_f(\alpha, q) = \Delta E(\alpha, q) + \sum n_i \mu_i + qE_F, \quad (1)$$

where $\Delta E(\alpha, q) = E(\alpha, q) - E(\text{SiC}) + \sum n_i E(i) + q\varepsilon_{VBM}$, where $E(\alpha, q)$ is the total energy of the SiC supercell containing the defect α at the charge state q, $E(\text{SiC})$ is the total energy of the SiC supercell, E_F is the Fermi energy referred the valence band maximum (VBM) of SiC, n_i is the number of atoms removed from or added into the supercell, and μ_i is the chemical potential of constituent i referred to elemental solid or gas with energy $E(i)$. In the case of charged defects, a charge correction to the formation energies is applied.[34]

Thermal-equilibrium conditions exert a series of thermodynamic limits on the achievable values of μ_i. First, the values of μ_i are limited to those values that maintain stable SiC,

$$\mu_{\text{Si}} + \mu_{\text{C}} = \Delta H_f(\text{SiC}). \quad (2)$$

Second, for the avoidance of the precipitation of Si, C, and Al, the values of μ_i are limited by

$$\mu_{\text{Si}} \leq 0, \ \mu_{\text{C}} \leq 0, \ \mu_{\text{Al}} \leq 0. \quad (3)$$

Finally, for the avoidance of the formation of secondary phases of Al_4C_3, the values of μ_i are limited by

$$4\mu_{\text{Al}} + 3\mu_{\text{C}} \leq \Delta H_f(\text{Al}_4\text{C}_3), \quad (4)$$

where $\Delta H_f(\text{Al}_4\text{C}_3)$ is the formation energy of Al_4C_3. Solving Eqs. (2)–(4), we obtain the accessible range for the values of μ_i, as shown by the green region in Fig. 1.

C. Carrier density calculations

Based on the formation energies and the electronic structures of defects, we use the detailed balance theory[26] to calculate the Fermi energy and carrier concentration of Al-doped 4H-SiC. The

11 April 2024 12:47:02

Published under an exclusive license by AIP Publishing

FIG. 1. Accessible range of chemical potentials (green region) for the thermal-equilibrium doping of Al in 4H-SiC.

concentrations of holes and electrons are calculated by using

$$p_0 = N_v e^{(E_v - E_F)/k_B T} = N_v e^{-E_F/k_B T}, \tag{5}$$

$$n_0 = N_c e^{-(E_c - E_F)/k_B T} = N_c e^{(E_F - E_g)/k_B T}, \tag{6}$$

where E_v and E_c are the energies of VBM and conduction-band minimum (CBM) of 4H-SiC, respectively. E_v are usually set to zero. E_g is the bandgap of SiC. k_B is the Boltzmann constant. N_v and N_c are the effective densities of states of the valence bands and conduction bands, respectively. N_v and N_c are given by

$$N_v = 2(2\pi m_p^* k_B T)^{3/2}/h^3, \tag{7}$$

$$N_c = 2(2\pi m_n^* k_B T)^{3/2}/h^3, \tag{8}$$

where m_p^* and m_n^* are the effective mass of holes (3.00 m_0, m_0 is the mass of free electron) and electrons (0.42 m_0), respectively. The charge neutrality condition requires that

$$p_0 + n_D^+ = n_0 + n_A^-. \tag{9}$$

Here, n_D^+ and n_A^- are the concentrations of positively charged donors and negatively charged acceptors, respectively. For ordinary doping conditions, the distribution of charged defects satisfies the Boltzmann distribution. For degenerate doping (i.e., the doping concentration exceeds N_V), the distribution of charged defects satisfies the Fermi–Dirac distribution. Hence, the concentration for a defect α with charge state q is calculated by the Boltzmann distribution or Fermi–Dirac distribution,

$$n(\alpha, q) = N_{site} g_q e^{-\Delta H_f(\alpha,q)/K_B T} \text{ (Boltzmann distribution)}, \tag{10}$$

$$n(\alpha, q) = N_{site} \frac{1}{1 + \frac{1}{g_q} e^{-\Delta H_f(\alpha,q)/K_B T}} \text{ (Fermi-Dirac distribution)}, \tag{11}$$

where N_{site} is the number of sites that may be occupied by the defect α per volume and g_q is the degeneracy factor that corresponds to the number of possible electron configurations. For degenerate p-type 4H-SiC, we use the Pearson–Bardeen model[1,17] to make corrections on the ionization energy [$\varepsilon(0/-)$] of Al by $\varepsilon(0/-) = 0.23 - \alpha(N_{Al})^{1/3}$, as shown in Fig. S1 in the supplementary material. In this case, the corrected formation energies of Al_{Si}^- are calculated by using

$$\begin{aligned} \Delta H_f(Al_{Si}^-) &= \Delta H_f(Al_{Si}^0) + \varepsilon(0/-) - E_F \\ &= \Delta H_f(Al_{Si}^0) + 0.23 - \alpha(N_{Al})^{1/3} - E_F. \end{aligned} \tag{12}$$

Figure S2 in the supplementary material shows an example of the correction of $\Delta H_f(Al_{Si}^-)$ of 4H-SiC with the Al concentration of $2.0 \times 10^{20}\ cm^{-3}$. By solving Eqs. (1) and (5)–(12) self-consistently, we can obtain the carrier concentrations, Fermi energies, and defect concentrations of Al-doped 4H-SiC at a given temperature and chemical potential.

III. RESULTS AND DISCUSSION

A. Formation energy

It is normally believed that Al is energy favorable located at the Si sublattice than the C sublattice. After substituting Si, it exhibits as an acceptor. However, whether it is energy favorable for Al located at the interstitial site is still unknown. Al at the interstitial site could be a potential compensating center. Moreover, the intrinsic defects in 4H-SiC also have the potential to compensate the holes. From the intrinsic defects, the carbon vacancy (V_C) exhibits the negative-U behavior, which can be a donor for p-type 4H-SiC. For the interstitial defects, C interstitials (C_i) and Si interstitials (Si_i) are also donors. Among V_C, C_i, and Si_i, V_C has the lowest formation energy, and the formation energies of V_{Si}, C_i, and Si_i are so large that their effects can be ignored. So, V_C has the biggest possibility to compensate Al-doped SiC. The interaction of V_C with aluminum acceptor is considered in this work. Gali *et al.*[46] show that V_C can be attached to the aluminum acceptor. The interaction of V_C with other defects is ignored. It has been reported that V_C can bind with V_{Si} or C_{Si} and form V_C–V_{Si} or V_C–C_{Si} complexes.[35–37] Compared with V_C, both V_C–V_{Si} and V_C–C_{Si} have much higher formation energy, which suggests that only a small part of V_C would form complexes.

As shown in Fig. 2(a), the defect configurations of Al in 4H-SiC considered in this work include interstitial Al (Al_i), substitutional Al at C-lattice sites (Al_C), and substitutional Al at Si lattice sites (Al_{Si}). For Al_i, four types of interstitial sites are considered. $Al_i^{C_te}$ and $Al_i^{Si_te}$ are the Al atoms located at the carbon- and silicon-coordinated tetrahedral sites, respectively. Al_i^{Si-C} is the Al atom located at the hexagonal layer accommodating an equally carbon- and silicon-coordinated site. Al_i^{hex} is the Al atom located at

11 April 2024 12:47:02

Published under an exclusive license by AIP Publishing

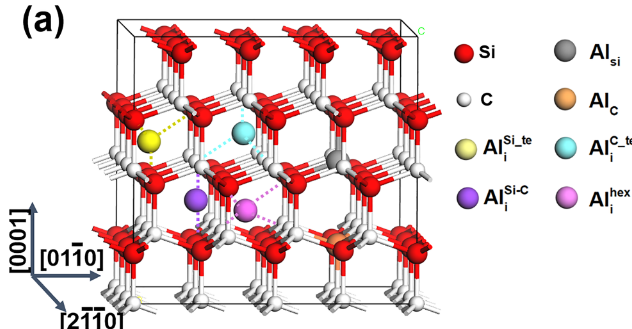

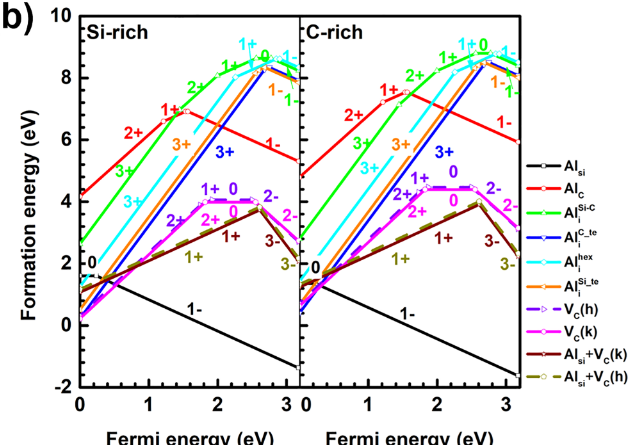

FIG. 2. (a) Optimized atomic structures of different defect configurations of Al in 4H-SiC. Defect configurations of Al_C, Al_{Si}, $Al_i^{C\text{–}te}$, $Al_i^{Si\text{–}te}$, Al_i^{Si-C}, and Al_i^{hex} are denoted by gray, orange, cyan, purple, pink, and yellow balls, respectively. Host lattice sites of Si and C are denoted by red and white balls, respectively. (b) Calculated defect formation energies of Al, V_C, and Al_{Si}–V_C at the Si-rich limit and C-rich limit.

the site encompassed by the upper and lower hexagonal basal plane. We note that the nonequivalent sublattice sites of Si and C in 4H-SiC include the quasihexagonal (h) and quasicubic (k) sites. When constructing Al_C (Al_{Si}), we substitute the lower-energy C (Si) at the k-site by Al.

The calculated formation energies of Al and V_C at the Si-rich limit (point A in Fig. 1) and the C-rich limit (point C in Fig. 1) are shown in Fig. 2(b). It is clear that substitutional Al in the Si lattice site is more energetically favorable than that in the C-lattice site. The calculated (0/−) transition energy of Al_{Si} is $E_V + 0.23$ eV, which well agrees with experiment results.[1] Among all possible interstitial sites, the formation energies of $Al_i^{C\text{–}te}$ are the lowest due to the steric effect. For p-type 4H-SiC, the 3+ charge state dominates the charge states of $Al_i^{C\text{–}te}$. It has been found that V_C is the dominant intrinsic defect in p-type 4H-SiC.[38–44] Therefore, we consider the compensation of V_C for the p-type doping of 4H-SiC. V_C acts as a negative-U center[36] in 4H-SiC. The (0/2−) transition levels of $V_C(h)$ and $V_C(k)$ are located at $E_v + 2.60$ and $E_v + 2.67$ eV, respectively. The (2+/0) transition level are located at $E_v + 1.84$ eV [$V_C(h)$] and $E_v + 1.90$ eV [$V_C(k)$]. It is well-known that the negative-U behavior does not occur to the charge transition level (+|0) of V_C at both inequivalent lattice sites.[37,38] In this calculation, the (+/0) level appears at $V_C(h)$ but not at $V_C(k)$, which could contribute to the Coulomb interaction between the charged defects in different cells. However, this may not influence the formation energy of the calculated defects and the result is still valid. V_C^{2-} and V_C^{2+} are the dominant types of V_C in n-type and p-type 4H-SiC, respectively. Therefore, $(Al_i^{C\text{–}te})^{3+}$ and V_C^{2+} need to be the most seriously considered for the compensation of p-type doping in Al-doped SiC. Moreover, Al vacancy-complexes are also taken into consideration. For all the complexes,[45,46] except Al_{Si}–V_C, the formation energy of the complexes is high. It is reasonable only Al_{Si}–V_C complexes are involved. Al_{Si}–V_C are in 1+ and 3− charge states, and the (1+/3−) transition level is located at $E_v + 2.61$ eV.

B. Carrier density

Using the calculated defect formation energies and the detailed balance theory, we calculate the Fermi energies as well as the concentrations of holes and defects as functions of the chemical potential of μ_C, which varies from point A to point C as shown in Fig. 1. μ_{Al} is set as the highest value in its accessible region. Since the growth temperature of 4H-SiC substrate is around 2400 K, we take this temperature to investigate the compensation in 4H-SiC together with the room temperature of 300 K.

At 2400 K, the value of N_V is 1.6×10^{21} cm^{-3}. Because the solubility of Al (from 4.5×10^{20} to 7.2×10^{20} cm^{-3} as μ_C varies from point A to point C) is less than N_V [Fig. 3(a)], we use the Boltzmann distribution to calculate the concentration of charged Al_{Si}. At 2400 K, the Fermi energy of 4H-SiC decreases from 0.69 to 0.46 eV with the increase of μ_C because of the decreased μ_{Si} that facilitates the formation of Al_{Si} acceptor. This indicates that the p-type doping of 4H-SiC can be enhanced by tuning the growth condition toward the C-rich condition. With the increase of μ_C, the hole concentration increases from 5.8×10^{19} to 1.8×10^{20} cm^{-3} [Fig. 3(a)]. The concentration of Al_{Si}^- is higher than that of holes by one order of magnitude, indicating that part of Al_{Si}^- is significantly compensated by intrinsic defects or is self-compensated. As shown in the bottom panel of Fig. 3(a), the calculated concentration of V_C^{2+} is as high as 2×10^{20} cm^{-3} and the concentration of $(Al_{Si}\text{–}V_C)^{1+}$ is 5×10^{19} cm^{-3}, while the concentration of Al_i^{3+} is ~1.0×10^{18} cm^{-3}. Therefore, it is the dominant compensation of V_C^{2+} and supplementary self-compensation of Al_i^{3+} that give rise to the limited hole concentration of Al in 4H-SiC. For example, under the Si-rich limit, the concentration of Al_{Si}^- is 5.4×10^{20} cm^{-3}, while the concentrations of V_C^{2+}, $(Al_{Si}\text{–}V_C)^{1+}$, and Al_i^{3+} are 1.6×10^{20}, 5.4×10^{19}, and 1.0×10^{18} cm^{-3}, respectively. This means that in this case, ~30.0% $((N_{V_C^{2+}} + N_{(Al_{Si}-V_C)^{1+}})/N_{Al_{Si}^-})$ of Al_{Si}^- is compensated by V_C^{2+}, while ~0.1% $(N_{Al_i^{3+}}/N_{Al_{Si}^-})$ of Al_{Si}^- is compensated by Al_i^{3+}.

When 4H-SiC is slowly cooled down to 300 K, the defect configurations and charge states have enough time to relax. Therefore, the concentrations of different defect configurations and charge states fully redistribute with the change of temperature. As 4H-SiC slowly cools down to 300 K, the amount of Al beyond the solution limit at 300 K will precipitate out. Eventually, At 300 K, the amount

11 April 2024 12:47:02

Published under an exclusive license by AIP Publishing

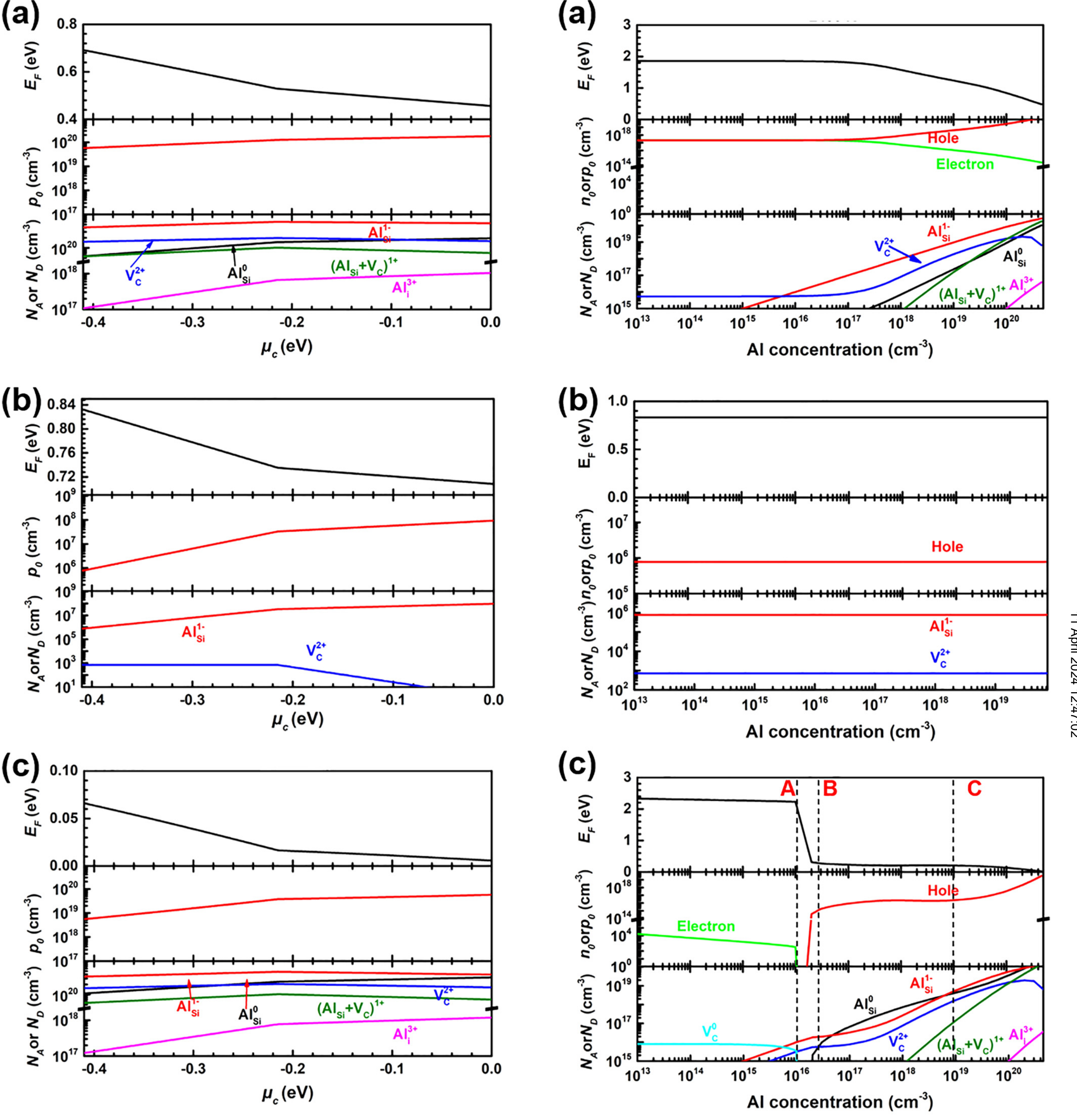

FIG. 3. Fermi energies (E_F), hole concentrations (p_0), and defect concentrations (N_A or N_D) of Al-doped 4H-SiC as functions of μ_C. (a) 4H-SiC is at the growth temperature of 2400 K. (b) 4H-SiC is slowly cooled down to the room temperature of 300 K. (c) 4H-SiC is quenched to the room temperature of 300 K.

FIG. 4. Calculated Fermi energies (E_F), electron or hole densities (n_0 or p_0), and defect concentrations (N_A or N_D) of Al-doped 4H-SiC as functions of the concentration of Al. (a) 4H-SiC is at the growth temperature of 2400 K. (b) 4H-SiC is slowly cooled down to the room temperature of 300 K. (c) 4H-SiC is quenched to the room temperature of 300 K.

11 April 2024 12:47:02

Published under an exclusive license by AIP Publishing

of Al still occupied on the Si lattice (Al_{Si}) is in the range of 7.8×10^5 to $9.3 \times 10^7\,cm^{-3}$ as μ_C varies from point A to point C. As shown in Fig. 3(b), Al_{Si} is in the Al_{Si}^- charge state and V_C is in the dominant V_C^{2+} charge state. The concentrations of Al_{Si}^- and V_C^{2+} decrease to be lower than $10^8\,cm^{-3}$. The thermally excited holes make the pinned Fermi energy of 4H-SiC change from 0.83 to 0.70 eV when the growth condition changes from the Si-rich limit to the C-rich limit [as shown in Fig. 3(b)].

When 4H-SiC is rapidly quenched to 300 K, the total concentrations of defects are assumed to remain unchanged, while the concentrations of defects at different charge states redistribute according to their weights.[47–50] The concentrations of thermally excited electrons and holes decrease due to the decreased temperature. At lower temperatures, the concentration of Al_{Si}^- becomes larger than the effective densities of states of the valence bands (N_V). Therefore, when 4H-SiC is rapidly quenched to 300 K, a degenerate p-type 4H-SiC is formed. The ionization energy [$\varepsilon(0/-)$] of Al decreases. We have used the Fermi–Dirac distribution to calculate the concentration of Al_{Si}^-. As shown in Fig. 3(c), when 4H-SiC is quenched from 2400 to 300 K, the concentrations of Al_{Si}^-, Al_i^{3+}, $(Al_{Si}–V_C)^{1+}$, and V_C^{2+} in 4H-SiC do not change significantly, giving rise to the decrease of the Fermi energy. This indicates that the p-type doping of SiC can be enhanced by quenching.

For Al-doped 4H-SiC at the growth temperature of 2400 K, V_C^{2+} is the dominant intrinsic defect. When the concentration of Al increases to the value larger than $10^{16}\,cm^{-3}$, i.e., the concentration of Al_{Si}^- is larger than the V_C^{2+}, the Fermi energy of SiC begins to decrease. With the decrease of the Fermi energy, the concentration of V_C^{2+} rapidly increases, which gives rise to the compensation of p-type doping in Al-doped 4H-SiC. Even if the concentration of Al increases to $4.5 \times 10^{20}\,cm^{-3}$, the Fermi energy of 4H-SiC is as high as 0.69 eV [Fig. 4(a)]. When 4H-SiC is slowly cooled down to 300 K because the doped concentration of Al at 2400 K exceeds the solid solubility limit ($7.8 \times 10^5\,cm^{-3}$) at 300 K, the excess Al will precipitate out and the concentration keeps at $7.8 \times 10^5\,cm^{-3}$. The Fermi energy is stabilized at 0.83 eV, while the concentration of Al_{Si}^- is $7.8 \times 10^5\,cm^{-3}$ and V_C^{2+} is $7.1 \times 10^2\,cm^{-3}$ [Fig. 4(b)].

When 4H-SiC is rapidly quenched to 300 K, even with the effective compensation of V_C^{2+}, the Fermi energy decreases sharply due to the charge redistribution [Fig. 4(c)]. For 4H-SiC with the concentration of Al smaller than $10^{16}\,cm^{-3}$, the thermally excited carriers pin the Fermi energy at ∼2.3 eV. In this case, the concentration of Al_{Si}^- is twice as large as that of V_C^{2+}, indicating that the holes of ionized Al_{Si}^- are totally compensated by V_C^{2+}. Once the concentration of Al increases to the value larger than the sum of V_C [point A as shown in Fig. 4(c)], the Fermi energy begins to decrease rapidly with the increase of the Al concentration. As the Al concentration increases from 1.0×10^{16} to $2.0 \times 10^{16}\,cm^{-3}$ (point A to point B as shown in Fig. 4), Al_{Si}^- is the dominant configuration of Al in 4H-SiC. The concentration of Al_{Si}^- becomes larger than the double of V_C^{2+}. This gives rise to the decrease of Fermi energy when the Al concentration increases from $1.0 \times 10^{16}\,cm^{-3}$ [point A as shown in Fig. 4(c)] to $2.0 \times 10^{16}\,cm^{-3}$ [point B as shown in Fig. 4(c)]. As the Al concentration further increases from $2.0 \times 10^{16}\,cm^{-3}$ [point B as shown in Fig. 4(c)] to $5.5 \times 10^{18}\,cm^{-3}$ [point C as shown in Fig. 4(c)], the charge redistribution of Al_{Si}

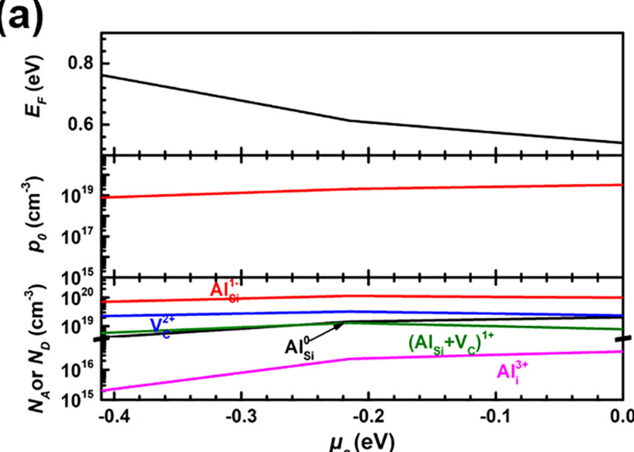

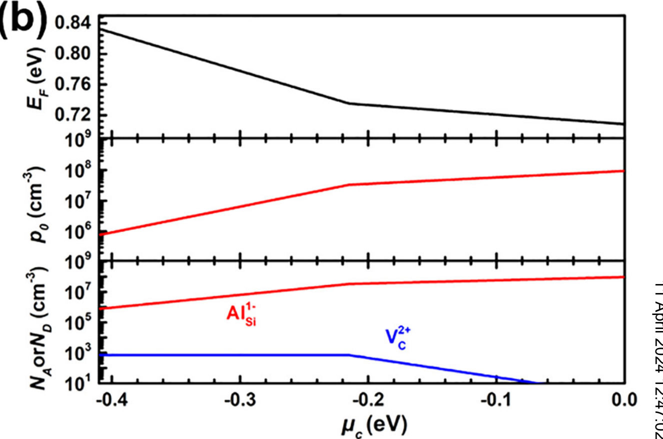

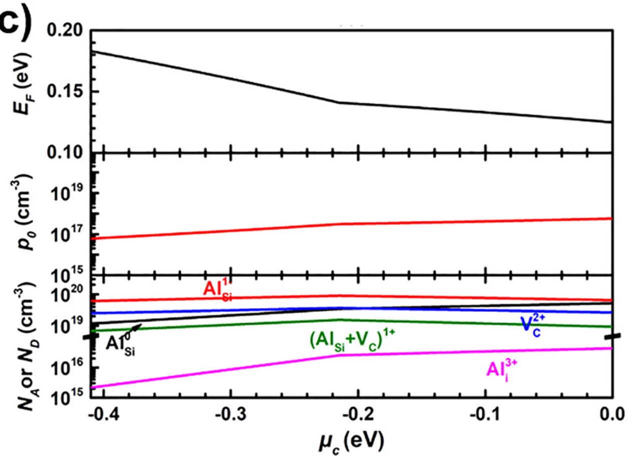

FIG. 5. Calculated Fermi energies (E_F), hole densities (p_0), and defect concentrations (N_A or N_D) of Al-doped 4H-SiC as functions of μ_C. (a) SiC is at the growth temperature of 1800 K. (b) SiC is slowly cooled down to the working temperature of 300 K. (c) SiC is quenched to the room temperature of 300 K.

11 April 2024 12:47:02

Published under an exclusive license by AIP Publishing

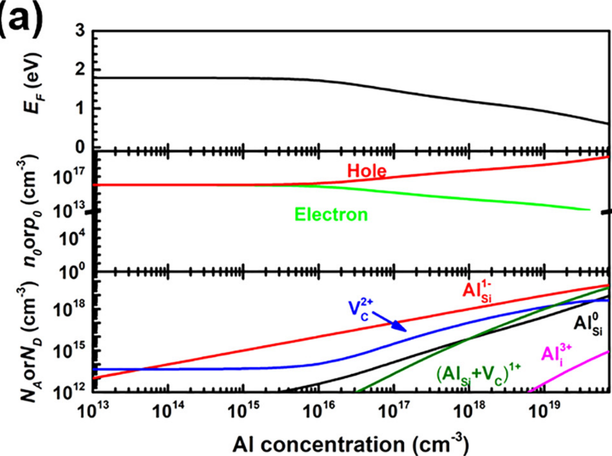

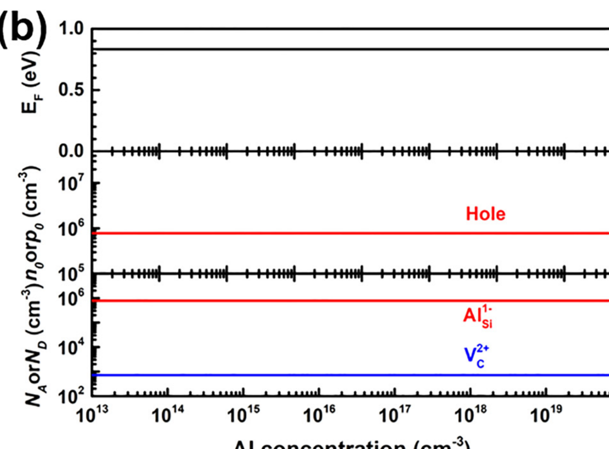

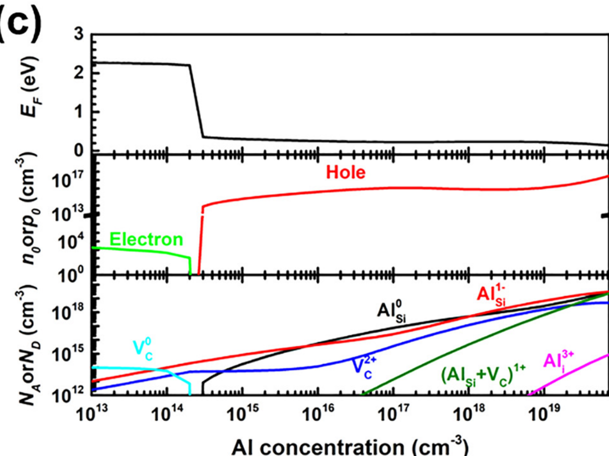

FIG. 6. Calculated Fermi energies (E_F), hole densities (p_0), and defect concentrations (N_A or N_D) of Al-doped 4H-SiC as functions of the concentration of Al. (a) SiC is at the growth temperature of 1800 K. (b) SiC is slowly cooled down to the working temperature of 300 K. (c) SiC is quenched to the room temperature of 300 K.

leads to the increase of the concentration of Al_{Si}^0. The concentration of Al_{Si}^0 becomes larger than Al_{Si}^-, but the concentration of Al_{Si}^- is still larger than that of V_C^{2+}. Therefore, the Fermi energy still decreases with the increase of the concentration of Al. When the concentration of Al exceeds 5.5×10^{18} cm^{-3}, the ionization energy [ε(0/−)] of Al sharply decreases, as shown in Fig. S1 in the supplementary material. This leads to the higher ionization rate of Al_{Si}. The concentration of Al_{Si}^- becomes larger than Al_{Si}^0. As the concentration of Al reaches 4.5×10^{20} cm^{-3}, the Fermi energy of 4H-SiC decreases to 0.14 eV if quenching takes place. It should be noted that even the compensation of V_C^{2+} plays an important role on the p-type doping of 4H-SiC with the Al concentration in the range from 1.0×10^{16} to 4.5×10^{20} cm^{-3}; quenching holds the potential of enhancing the p-type doping in Al-doped 4H-SiC.

We have also studied the Fermi energies, electron/hole concentrations, and defect concentrations as functions of the chemical potential (the concentration of Al) at the temperature of 1800 K and for quenching from 1800 to 300 K because the epitaxial growth temperature of 4H-SiC is around 1800 K. The results are shown in Figs. 5 and 6. The dominant compensation of V_C^{2+} is also found. The Fermi energy of 4H-SiC grown at 1800 K is lower than that of 4H-SiC grown at 2400 K, as a result of the decreased concentration of ionized Al_{Si} at a lower temperature.

We now take 4H-SiC substrate (epilayer) grown at 2400 K (1800 K) under the Si-rich condition (point A in Fig. 1) and its use at 300 K as an example to evaluate the hole concentration of Al in 4H-SiC. For the 4H-SiC substrate (epilayer), the solubility limit of Al is 4.5×10^{20} cm^{-3} (7.3×10^{19} cm^{-3}). The calculated hole concentration of the 4H-SiC substrate (epilayer) is 7.8×10^{19} cm^{-3} (6.1×10^{18} cm^{-3}). The mobility of holes (μ_p) of the 4H-SiC substrate (epilayer) is 2.8 cm^2 V^{-1} s^{-1} (9.3 cm^2 V^{-1} s^{-1}), which is obtained by using[1]

$$\mu_p = \frac{118}{1 + [(N_A + N_D)/2.2 \times 10^{18}]^{0.7}}. \tag{13}$$

The resistivity of the 4H-SiC substrate (epilayer) is then 0.028 Ω cm (0.11 Ω cm). Compared with the 4H-SiC substrate from solution growth, the calculated resistivity of the 4H-SiC substrate is in the same order of magnitude.[24,25] However, as for the epilayer, there exists a large difference between the calculated value and the experimental value. This is because dopant incorporation during epitaxial growth is kinetic controlled and solubility limits may be exceeded.[51,52] The Al doping concentration can reach up to ∼5×10^{20} cm^{-3} with a resistance of ∼0.016 Ω cm.[53,54] Moreover, the compensation concentration of V_C is very low and its compensation effect on Al can be mostly ignored. It found that the concentration of compensating defects in Al-doped 4H-SiC epilayers is very low (only <1% of the Al concentration).[27,55] This is because that the concentration of V_C of 4H-SiC epilayers is strongly dependent on the C/Si ratio and growth temperature. Through adjusting the C/Si ratio and growth temperature, the concentration of V_C can be controlled in a low level.[56]

Since the resistivity of 4H-SiC is mainly limited by the compensation of V_C^{2+}, the passivation of V_C^{2+} is highly desired to enhance the hole concentration of 4H-SiC. We may evaluate the possible improvement of the hole concentration of Al in 4H-SiC if

11 April 2024 12:47:02

Published under an exclusive license by AIP Publishing

V_C is properly passivated. For the SiC substrate (epilayer) with the Al concentration reaching the solubility limit of $4.5 \times 10^{20}\ \mathrm{cm}^{-3}$ ($7.3 \times 10^{19}\ \mathrm{cm}^{-3}$), the Fermi energy is pinned at 0.06 eV (0.18 eV) due to the compensation of V_C^{2+} even if rapid quenching is used. If V_C is properly passivated, however, the Fermi energy decreases to 0.04 eV (0.1 eV) [Fig. 7]. With this passivation of V_C, the hole concentration of Al in 4H-SiC substrate (epilayer) increases from 1.24% (0.1%) to 6.82% (4.8%). By combining the passivation of V_C and quenching approach, the resistivity of the 4H-SiC substrate (epilayer) may decrease to 12 m Ω cm (51 m Ω cm). If the compensation of Al_i^{3+} is additionally removed, the hole concentration of Al in the 4H-SiC substrate (epilayer) increases to 9.6% (5.3%). The resistivity of the 4H-SiC substrate (epilayer) further decreases to 9 m Ω cm (48 m Ω cm).

FIG. 7. Comparison of Fermi energies (E_F), hole densities (p_0), doping efficiencies (p_0/N_{Al}), and resistivities (R) of Al doping SiC with the compensation of both V_C^{2+} and self-compensation ($V_C^{2+} + Al_i^{3+}$), with only self-compensation (Al_i^{3+}), and without any compensating centers (compensation-free).

IV. CONCLUSION

In conclusion, we have systematically investigated the compensation of native defects and self-compensation in Al-doped 4H-SiC. It has been found that V_C^{2+} are the dominant compensating centers in Al-doped 4H-SiC. When the concentration is in the range of 10^{16}–$10^{19}\ \mathrm{cm}^{-3}$, the concentration of holes is lower by one order of magnitude than the Al concentration because of the compensation of V_C^{2+}. As the Al concentration exceeds $10^{20}\ \mathrm{cm}^{-3}$, the concentration of holes is only in the order of magnitude of $10^{19}\ \mathrm{cm}^{-3}$ owing to the dominant compensation of V_C^{2+} and supplementary self-compensation of Al_i^{3+}. The current work on the elucidation of the compensation of *p*-type doping in 4H-SiC should encourage the development of practical methods to remove the compensation of V_C^{2+} and quench 4H-SiC, realizing Al-doped 4H-SiC with very low resistivity.

SUPPLEMENTARY MATERIAL

See the supplementary material for Figs. S1 and S2.

ACKNOWLEDGMENTS

This work was supported by the National Key Research and Development Program of China (Grant No. 2018YFB2200101), the Natural Science Foundation of China (Grant Nos. 91964107 and U20A20209) and the "Pioneer" and "Leading Goose" R&D Program of Zhejiang (Grant No. 2022C01021). Partial support from the Natural Science Foundation of China for Innovative Research Groups (Grant No. 61721005) is also acknowledged. The National Supercomputer Center in Tianjin is acknowledged for computational support.

11 April 2024 12:47:02

AUTHOR DECLARATIONS

Conflict of Interest

The authors have no conflicts to disclose.

DATA AVAILABILITY

The data that support the findings of this study are available within the article and its supplementary material.

REFERENCES

[1] T. Kimoto and J. A. Cooper, *Fundamentals of Silicon Carbide Technology: Growth, Characterization, Devices and Applications* (John Wiley & Sons, 2014).
[2] F. F. Wang and Z. Zhang, CPSS Trans. Power Electron. Appl. **1**, 13 (2016).
[3] F. Roccaforte, P. Fiorenza, G. Greco, R. Lo Nigro, F. Giannazzo, F. Iucolano, and M. Saggio, Microelectron. Eng. **187–188**, 66 (2018).
[4] J. H. Zhao, P. Alexandrov, and X. Li, IEEE Electron Device Lett. **24**, 402–404 (2003).
[5] T. Hatakeyama and T. Shinohe, Mater. Sci. Forum **389–393**, 1169–1172 (2002).
[6] N. Ren, J. Wang, and K. Sheng, IEEE Trans. Electron Devices **61**, 2459 (2014).
[7] H. Li, J. Wang, N. Ren, H. Xu, and K. Sheng, Micromachines **10**, 485 (2019).
[8] J. Wang, T. Zhao, J. Li, A. Q. Huang, R. Callanan, F. Husna, and A. Agarwal, IEEE Trans. Electron Devices **55**(8), 1798–1806 (2008).
[9] K. Cha and K. Kim, J. Semicond. **42**, 062801 (2021).
[10] X. Luo, K. Zhang, X. Song, J. Fang, F. Yang, and B. Zhang, J. Semicond. **41**, 102801 (2020).

Published under an exclusive license by AIP Publishing

[11]T. Zhao, J. Wang, A. Q. Huang, and A. Agarwal, in *IEEE Industry Applications Annual Meeting* (IEEE, 2007), p. 331.
[12]A. Kadavelugu and S. Bhattacharya, in *IEEE Applied Power Electronics Conference and Exposition-APEC 2014* (IEEE, 2014), p. 1494.
[13]L. Han, L. Liang, Y. Kang, and Y. Qiu, IEEE Trans. Power Electron. **36**, 2080 (2021).
[14]A. Kadavelugu, S. Bhattacharya, S. H. Ryu, E. Van Brunt, D. Grider, A. Agarwal, and S. Leslie, in *IEEE Energy Conversion Congress and Exposition* (IEEE, 2013), p. 2528.
[15]X. Wang and J. A. Cooper, IEEE Trans. Electron Devices **57**, 511 (2010).
[16]R. Müller, U. Künecke, R. Weingärtner, H. Schmitt, P. Desperrier, and P. J. Wellmann, Mater. Sci. Forum **483–485**, 31 (2005).
[17]T. Shirai, K. Danno, A. Seki, H. Sakamoto, and T. Bessho, Mater. Sci. Forum **778-780**, 75 (2014).
[18]Z. Zhang, L. Chen, J. Deng, G. Wang, Y. Song, J. Guo, and X. Chen, Appl. Phys. A **126**, 1 (2020).
[19]K. Eto, T. Kato, S. Takagi, T. Miura, Y. Urakami, H. Kondo, and H. Okumura, Mater. Sci. Forum **821–823**, 47 (2015).
[20]K. Eto, H. Suo, T. Kato, and H. Okumura, Mater. Sci. Forum **858**, 77 (2016).
[21]K. Eto, H. Suo, T. Kato, and H. Okumura, J. Cryst. Growth **470**, 154 (2017).
[22]X. Xie, L. Sun, X. Chen, X. Yang, X. Hu, and X. Xu, Scr. Mater. **167**, 76 (2019).
[23]Y. C. Huang, R. Wang, Y. X. Qian, Y. Q. Zhang, D. Yang, and X. D. Pi, Chin. Phys. B **31**, 046104 (2022).
[24]C. Darmody and N. Goldsman, J. Appl. Phys. **126**, 145701 (2019).
[25]M. Krieger, K. Semmelroth, and G. Pensl, Mater. Sci. Forum **457–460**, 685 (2004).
[26]S. Contreras, M. Zielinski, L. Konczewicz, C. Blanc, S. Juillaguet, R. Müller, and J. Camassel, Mater. Sci. Forum **527-529**, 633 (2006).
[27]S. Asada, T. Okuda, T. Kimoto, and J. Suda, Appl. Phys. Express **9**, 041301 (2016).
[28]Y. Negoro, T. Kimoto, H. Matsunami, F. Schmid, and G. Pensl, J. Appl. Phys. **96**, 4916 (2004).
[29]R. Nipoti, R. Scaburri, A. Hallén, and A. Parisini, J. Mater. Res. **28**, 17 (2013).
[30]J. Weiße, M. Hauck, M. Krieger, A. J. Bauer, and T. Erlbacher, AIP Adv. **9**, 055308 (2019).
[31]G. Kresse and J. Hafner, Phys. Rev. B **47**, 558 (1993).
[32]S. H. Wei, Comput. Mater. Sci. **30**, 337 (2004).
[33]R. Wang, X. Tong, J. Xu, S. Zhang, P. Zheng, F. X. Chen, and W. Tan, Phys. Rev. Appl. **11**, 054021 (2019).
[34]C. Freysoldt, J. Neugebauer, and C. G. Van deWalle, Phys. Rev. Lett. **102**, 016402 (2009).
[35]L. Torpo, T. E. M. Staab, and R. M. Nieminen, Phys. Rev. B **65**, 085202 (2002).
[36]A. Beste, D. E. Taylor, D. A. Golter, and C. W. Lai, Phys. Rev. B **98**, 214107 (2018).
[37]M. Bockstedte, A. Mattausch, and O. Pankratov, Phys. Rev. B **68**, 205201 (2003).
[38]X. Yan, P. Li, L. Kang, S. H. Wei, and B. Huang, J. Appl. Phys. **127**, 085702 (2020).
[39]N. T. Son, X. T. Trinh, L. S. Løvlie, B. G. Svensson, K. Kawahara, J. Suda, T. Umeda, J. Isoya, T. Makino, T. Ohshima, and E. Janzén, Phys. Rev. Lett. **109**, 187603 (2012).
[40]I. Capan, T. Brodar, Z. Pastuović, R. Siegele, T. Ohshima, S.-i. Sato, T. Makino, L. Snoj, V. Radulović, J. Coutinho, V. J. B. Torres, and K. Demmouche, J. Appl. Phys. **123**, 161597 (2018).
[41]T. Umeda, Y. Ishitsuka, J. Isoya, N. T. Son, E. Janzén, N. Morishita, T. Ohshima, H. Itoh, and A. Gali, Phys. Rev. B **71**, 193202 (2005).
[42]J. Coutinho, V. J. B. Torres, K. Demmouche, and S. Öberg, Phys. Rev. B **96**, 174105 (2017).
[43]A. Gali, B. Aradi, P. Deák, W. J. Choyke, and N. T. Son, Phys. Rev. Lett. **84**, 4926 (2000).
[44]L. Gordon, A. Janotti, and C. G. Van de Walle, Phys. Rev. B **92**, 045208 (2015).
[45]E. Igumbor, O. Olaniyan, R. E. Mapasha, H. T. Danga, E. Omotoso, and W. E. Meyer, Mater. Sci. Semicond. Process. **89**, 77 (2019).
[46]A. Gali, T. Hornos, N. T. Son, E. Janzén, and W. J. Choyke, Phys. Rev. B **75**, 045211 (2007).
[47]S. H. Wei and S. B. Zhang, Phys. Rev. B **66**, 155211 (2002).
[48]J. Ma, S. H. Wei, T. A. Gessert, and K. K. Chin, Phys. Rev. B **83**, 245207 (2011).
[49]B. Dou, Q. Sun, and S. H. Wei, Phys. Rev. Appl. **15**, 054045 (2021).
[50]J. H. Yang, J. S. Park, J. Kang, W. Metzger, T. Barnes, and S. H. Wei, Phys. Rev. B **90**, 245202 (2014).
[51]D. J. Larkin, P. G. Neudeck, J. A. Powell, and L. G. Matus, Appl. Phys. Lett. **65**, 1659 (1994).
[52]M. K. Linnarsson, M. S. Janson, U. Zimmermann, B. G. Svensson, P. O. Å Persson, L. Hultman, J. Wong-Leung, S. Karlsson, A. Schöner, H. Bleichner, and E. Olsson, Appl. Phys. Lett. **79**, 2016 (2001).
[53]S. Ji, K. Kojima, Y. Ishida, S. Saito, T. Kato, H. Tsuchida, and H. Okumura, J. Cryst. Growth **380**, 85 (2013).
[54]S. Ji, K. Eto, S. Yoshida, K. Kojima, Y. Ishida, S. Saito, and H. Okumura, Appl. Phys. Express **8**, 121302 (2015).
[55]W. J. Choyke, H. Matsunami, and G. Pensl, *Silicon Carbide: Recent Major Advances* (Springer Science & Business Media, 2013).
[56]T. Kimoto, K. Hashimoto, and H. Matsunami, Jpn. J. Appl. Phys. **42**, 7294 (2003).

11 April 2024 12:47:02

Published under an exclusive license by AIP Publishing